One-Dimensional Model of Vacuum Filtration of Compressible Flocculated Suspensions

Anthony D. Stickland, Ross G. de Kretser, and Peter J. Scales
Dept. of Chemical and Biomolecular Engineering, Particulate Fluids Processing Centre, The University of Melbourne, VIC 3010, Australia

DOI 10.1002/aic.12194
Published online February 1, 2010 in Wiley Online Library (wileyonlinelibrary.com).

This work details the one-dimensional modeling of the different processes that may occur during the vacuum filtration of compressible flocculated suspensions. Depending on the operating conditions of the applied pressure and the initial solids concentration relative to the material properties of the compressive yield stress and the effective capillary pressure at the air–liquid interface, the dewatering process undergoes a combination of cake formation, consolidation, and/or desaturation. Mathematical models for these processes based on the compressional rheology approach are presented and appropriate solution methods outlined. Results using customary material properties are given for different operating conditions to illustrate the three dewatering processes. This approach lays the theoretical basis for further work understanding two- and three-dimensional effects during desaturation, such as cracking and wall detachment.
 AIChE J, 56: 2622–2631, 2010
Keywords: compressional rheology, solid/liquid separations, vacuum filtration, mathematical modeling, suspensions

Introduction

Vacuum filtration of flocculated suspensions is a common industrial dewatering process. In horizontal belt and rotary drum vacuum filters, for example, cakes are formed on semipermeable membranes that are subsequently consolidated and desaturated due to the applied vacuum pressure. Accurate prediction of such processes allows optimization of the throughput and final solids concentration of the product. This improves the efficiency of existing operations, provides a basis for design of new equipment, and gives improvements and cost reductions in ensuing processes such as the incineration of wastewater treatment sludge cake or spray drying of food starch, for example. In the laboratory, vacuum filtration is used to study the more general case of cake drainage behavior.

This work presents a model of one-dimensional vacuum filtration in which a vacuum pressure, Δp, is applied to a flocculated suspension of initial solids volume fraction ϕ_0 and initial height h_0 that is constrained by a semipermeable membrane at $z = 0$ (see Figure 1). The vacuum filtration of flocculated suspensions will undergo any or all of the three processes depending on the values of Δp and ϕ_0 relative to specific material properties—the two saturated processes of cake formation and cake consolidation followed by cake desaturation (or drainage).

Previously unpublished transient results for the vacuum filtration of calcium carbonate (Omyacarb® 2-LU, Omya California) at a constant pressure of 60 kPa are shown in Figure 2 to illustrate these different processes. The volume of filtrate as a function of time is plotted as V^2 vs. t, showing linear cake formation up to ~4200 s followed by logarithmic decay during cake consolidation up to 5000 s. There is an abrupt change in the gradient when cake desaturation begins—the slope increases briefly before decaying again, indicating multiple mechanisms involved in the desaturation process.

As discussed below, a model of vacuum filtration that includes cake consolidation and incorporates fundamentally sound desaturation physics (with cracking and wall detachment) is required. As a first step, this theoretical work presents a one-dimensional mathematical model for vacuum

Correspondence concerning this article should be addressed to A. D. Stickland at stad@unimelb.edu.au.

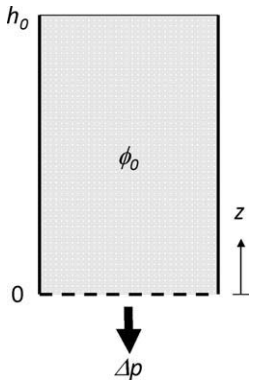

Figure 1. One-dimensional vacuum filtration.

filtration of compressible particulate suspensions based on the phenomenological theory developed by Buscall and White.[1] This approach is often termed "compressional rheology." Compressible flocculated suspensions of solids volume fraction, ϕ, are described as yield stress materials that exhibit network strength at concentrations above the gel point, ϕ_g.[1] The network consolidates locally if an applied pressure exceeds the compressive yield stress, $p_y(\phi)$, at a rate determined by the hindered settling function, $R(\phi)$. The saturated equilibrium solids concentration, ϕ_∞, is given by $\Delta p = p_y(\phi_\infty)$. Compressional rheology has been used successfully to model the saturated processes of thickening,[2,3] filtration,[4,5] and centrifugation[6–8] for flocculated slurries. In particular, the filtration model of Landman and White[9] is used here to describe the saturated processes of cake formation and cake consolidation.

During air-driven dewatering processes, particulate networks also exhibit an effective capillary pressure at the air–liquid interface due to surface tension and pore curvature. If the applied pressure exceeds the maximum effective capillary pressure that can be exerted, $p_{cap}^{max}(\phi)$, the network will desaturate and the air–liquid interface will recede into the porous solid.[10] Thus there are two competing mechanisms during dewatering using an air pressure gradient, consolidation and desaturation, compared with just consolidation if a piston is used to compress a particulate network.

The desaturation process involves the movement of a fluid front at $z_f(t)$ through the particulate network due to the applied pressure. For $z \leq z_f(t)$, the network is completely saturated. For $z > z_f(t)$, the network is partially desaturated. A residual amount of fluid will remain in the partially desaturated solid due to capillary condensation (that is, fluid is left behind at point contacts between particles), which is a function of the local solids concentration. The receding fluid front approach has been used to model consolidation and drainage during drying[11,12] and centrifugal filtration of suspensions.[7,8]

This continuum description of desaturation is how a particulate network would be expected to behave provided that the network structure that governs the desaturation is the same as that which governs the saturated cake formation and consolidation. However, it does not consider the two- and three-dimensional effects on the desaturating body of cracking or wall detachment, which can be vitally important for predicting the rate and extent of dewatering, nor fluid movement through the desaturated body due to gravitational drainage or percolation. What this work does do is provide a basis for further understanding of what happens when the body cracks by separating the expected behavior for the different process that may occur during vacuum filtration. Most importantly, it allows prediction of the critical concentration at which desaturation can begin.

Existing semiempirical models of cake desaturation during vacuum filtration, such as the work of Wakeman,[13] Baluais et al.,[14] and Nicolaou and Stahl,[15] describe incompressible particulate networks as bundles of capillaries that selectively desaturate with increasing pressure above a critical breakthrough pressure. Both air and liquid flow through the partially desaturated body at rates given by a modified Darcy's law for two-phase flow. The air-flow can be rate determining for low flow-rate systems.[16] While these approaches have proved useful in describing the long term desaturation kinetics for incompressible systems, they do not consider the consolidation of compressible cakes, such that the cake may shrink or have a volume fraction distribution, and they don't explain the initial increasing filtration rate at the initiation of desaturation (as illustrated in Figure 2).

An interesting aspect in these models is that the decrease in equilibrium saturation with increasing pressure is attributed to the desaturation of progressively smaller capillaries. The argument is actually the reverse case of mercury injection porosimetry—due to the nonwetting properties of mercury, it is necessary to apply a pressure to the mercury to make it enter a porous solid such that the incremental volume of mercury taken up by the solid as the pressure is increased allows determination of the pore size distribution.[17] However, the reverse argument for desaturation of a wetting fluid from a porous solid does not apply. Rather than more liquid being displaced as progressively smaller capillaries desaturate, no more capillaries will desaturate once the largest capillary is desaturated.

In addition, the underlying conceptual analogy is misleading. Particulate networks do not contain continuous capillaries of a fixed radius but interconnected tortuous paths (this

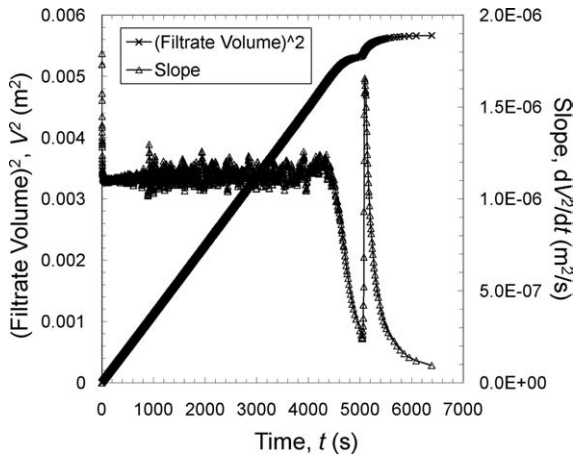

Figure 2. Constant pressure vacuum filtration results of volume of filtrate (V^2) and slope (dV^2/dt) vs. time for calcium carbonate at 60 kPa.

is recognized by most researchers and methods have been developed to extend the capillary analogy to particulate networks). The analogy does work well for saturated kinetics of incompressible materials but does not extend to desaturation due to the three-dimensional interconnectedness of the network and the partially saturated pores. Pore-scale models that describe gravitational fluid drainage and imbibition (percolation theory,[18–21] for example) are beyond the scope for this work but may be included at a later stage to improve the prediction of desaturation rates and residual saturation. The work presented here is a continuum model, not a capillary model, and references to drainage in this text refer to drainage from the entire body rather than at the pore-scale.

Theory

The vacuum filtration of flocculated suspensions will undergo any or all of cake formation, consolidation, and desaturation depending on the values of Δp and ϕ_0 relative to the material properties of $p_y(\phi)$ and $p_{cap}^{max}(\phi)$. $p_y(\phi)$ is generally described by a power-law function of ϕ with a high index,[22] whereas $p_{cap}^{max}(\phi)$ is generally of the order of ϕ.[10] The two functions intercept at the critical concentration, ϕ_{cap} (designated as ϕ_e by Brown and Zukoski[11]), which determines whether a cake will consolidate or desaturate. Below ϕ_{cap}, a pressure gradient causes the local network to collapse whereas, above ϕ_{cap}, the network desaturates.

The range of possible processes and their dependence on ϕ_0 and Δp is illustrated in Figure 3:

- If $\phi_0 < \phi_g$ (Case 1), the initial suspension is un-networked such that the application of a pressure causes a cake to form on the membrane. Once all the solids are in the cake, it consolidates until the solids pressure at the top either equals $p_y(\phi_{cap})$ [$\Delta p \geq p_y(\phi_{cap})$, Case 1(a)] or Δp [($\Delta p < p_y(\phi_{cap})$, Case 1(b)]. The cake then desaturates for Case 1(a);
- If $\phi_g \leq \phi_0 < \phi_{cap}$ (Case 2), the initial suspension is networked and the applied pressure causes it to consolidate until $\phi[h(t),t]$ either equals ϕ_{cap} [Case 2(a)] or ϕ_∞ [Case 2(b)]. The cake then desaturates for Case 2(a); and
- If $\phi_0 \geq \phi_{cap}$ (Case 3), $p_{cap}^{max}(\phi)$ is $<p_y(\phi)$, such that an applied pressure causes desaturation immediately. When $\Delta p > p_y(\phi_0)$ [Case 3(a)], the cake consolidates and desaturates concurrently. When $p_{cap}^{max}(\phi_0) < \Delta p < p_y(\phi_0)$ [Case 3(b)], the solids in the cake are immobile and only drainage occurs. Case 3(b) corresponds to the desaturation of incompressible cakes.

Solid–liquid conservation equations

Gravity can be ignored during formation and consolidation if the sedimentation rate is significantly slower than the filtration rate, as indicated by their relative time scales, T_{filt} and T_{sed}[9]:

$$\frac{T_{filt}}{T_{sed}} \approx \frac{\Delta\rho g \phi_0 h_0}{\Delta p} \frac{R(\phi_\infty)}{R(\phi_0)} \left(\frac{1-\phi_0}{1-\phi_\infty}\right)^2 \tag{1}$$

where $\Delta\rho$ is the density difference between the solid and liquid phases and g is the gravitational acceleration.

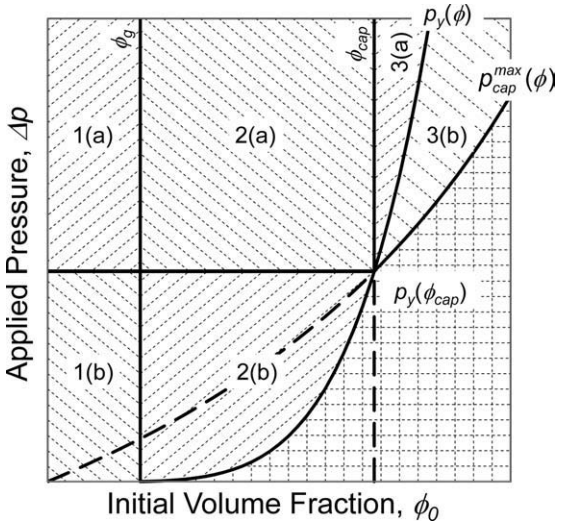

Figure 3. Diagram illustrating the processes during vacuum filtration of particulate suspensions due to volume fraction dependencies of compressive yield stress and maximum capillary pressure.

It is assumed here that the applied pressure or vacuum is always significant relative to gravity, therefore with negligible gravity, the conservation of momentum for the solid phase of a volume element of saturated suspension at position z and time t is[9]:

$$\frac{\partial p_s}{\partial z} = \frac{\phi R(\phi)}{(1-\phi)^2}\left(u - \frac{dv}{dt}\right) \tag{2}$$

where p_s is the local solids pressure, u is the local solids velocity, and dv/dt is the specific filtrate rate. Assuming that the dynamic compressibility is large such that p_s equals $p_y(\phi)$,[1] Eq. 2 becomes:

$$\frac{\partial \phi}{\partial z} = \frac{\phi}{D(\phi)}\left(u - \frac{dv}{dt}\right) \tag{3}$$

where the solids diffusivity, $D(\phi)$, is defined as:

$$D(\phi) = \frac{dp_y(\phi)}{d\phi}\frac{(1-\phi)^2}{R(\phi)} \tag{4}$$

The conservation of solids volume is:

$$\frac{\partial(\phi u)}{\partial z} = \frac{\partial \phi}{\partial t} \tag{5}$$

The initial conditions are:

$$\begin{aligned} \phi(z,0) &= \phi_0 \\ h(0) &= h_0 \end{aligned} \tag{6}$$

The membrane is assumed to be impervious to the solid phase, such that the overall conservation of solids volume is:

$$\int_0^{h(t)} \phi(z,t)dz = \phi_0 h_0 \tag{7}$$

In this work, the membrane resistance is assumed to be orders of magnitude lower than the cake resistance. Significant membrane resistance only affects the rate, not the extent of dewatering. Therefore, ignoring the membrane resistance does not change the conclusions of this work. In addition, it is easily incorporated if so desired. When the membrane resistance is negligible, the consolidation equations are scaled using the following parameters:

$$Z = \frac{z}{h_0} \quad H(T) = \frac{h(t)}{h_0} \quad V(T) = \frac{v(t)}{h_0} \quad T = \frac{D_\infty}{h_0^2}t \quad \psi = \frac{h_0}{D_\infty}\phi u$$
$$P = \frac{p}{\Delta p} \quad \Delta(\phi) = \frac{D(\phi)}{D_\infty} \quad B(\phi) = \frac{D_\infty}{\Delta p}\frac{R(\phi)}{(1-\phi)^2} \tag{8}$$

where D_∞ is $D(\phi_\infty)$. Notice that the time scales with h_0^2/D_∞. Doubling the initial height quadruples the filtration time with obvious consequences for the optimization of filter throughput. The time is inversely proportional to the diffusivity, such that materials with high diffusivities dewater quicker.

From Eq. 2, the scaled solids pressure gradient is:

$$\frac{\partial P_s}{\partial Z} = B(\phi)\left(\psi - \phi\frac{dV}{dT}\right) \tag{9}$$

From Eqs. 3 and 5, the local scaled concentration and flux gradients are:

$$\frac{\partial \phi}{\partial Z} = \frac{1}{\Delta(\phi)}\left[\psi - \phi\frac{dV}{dT}\right] \tag{10}$$

$$\frac{\partial \psi}{\partial Z} = \frac{\partial \phi}{\partial T} \tag{11}$$

Case 1: cake formation ($\phi_0 < \phi_g$)

If $\phi_0 < \phi_g$, the application of an applied pressure causes a cake of scaled height $Z_c(T)$ to form on the semipermeable membrane. The solids volume fraction in the cake varies from ϕ_∞ at the membrane (assuming that membrane resistance is insignificant) to ϕ_g at the top of the cake. Material above the cake $[Z_c(T) < Z < H(T)]$ remains at ϕ_0. Cake formation proceeds until all the solid material is in the cake [that is, $Z_c(T) = H(T)$] at time T_F. The boundary conditions for $0 \le T \le T_F$ are therefore[23]:

$$\phi(0,T) = \phi_\infty \quad \left.\frac{\partial \phi}{\partial Z}\right|_0 = -\phi_\infty \frac{dV}{dT}$$
$$\phi(Z_c,T) = \phi_g \quad \left.\frac{\partial \phi}{\partial Z}\right|_{Z_c} = -\frac{\phi_g - \phi_0}{\Delta(\phi_g)}\left(\frac{dV}{dT} + \frac{dZ_c}{dT}\right) \tag{12}$$

The exact solution until T_F is given by a similarity solution.[23] ϕ is scaled to the void ratio, $e(w,T)$ and $E(X)$, Z is scaled to the material coordinate, $w(Z,T)$, T is scaled to τ, and $\Delta(\phi)$ is scaled to $\delta(e)$ as defined by:

$$e(w,\tau) = \frac{1}{\phi(Z,T)} + 1 = \begin{Bmatrix} E(X) & w \le w_c(\tau) \\ e_0 & w > w_c(\tau) \end{Bmatrix} \tag{13}$$

$$X(w,\tau) = w\sqrt{\frac{\tau}{\tau_F}} \text{ where } w(Z,T) = \frac{1}{\phi_0}\int_0^Z \phi(Z,T)dZ \tag{14}$$

$$\tau = T\left(\frac{\phi_\infty}{\phi_0}\right)^2 \tag{15}$$

$$\delta(e) = \frac{\phi^2}{\phi_\infty^2}\Delta(\phi) \tag{16}$$

$X(w,\tau)$ is the similarity variable. Substituting these variables into Eqs. 10 and 11 and simplifying gives the following nonlinear ordinary differential equation for $E(X)$:

$$-\frac{X}{2\tau_F}\frac{dE}{dX} = \frac{d}{dX}\left(\delta(E)\frac{dE}{dX}\right) \tag{17}$$

The appropriate boundary conditions, from Eq. 12, are:

$$E(0) = e_\infty \tag{18}$$

$$E(1) = e_g \tag{19}$$

$$\left.\frac{dE}{dX}\right|_1 = \frac{e_0 - e_g}{2\tau_F \delta(e_g)} \tag{20}$$

$E(X)$ is determined by solving Eq. 17 using a 4th-5th order Runge-Kutta numerical method[24] from $X = 1$ to $X = 0$ for successive estimates of τ_F until Eq. 18 is satisfied. The cake height at the end of formation, H_F, is given by the cumulative void ratio:

$$H_F = \phi_0\left(1 + \int_0^1 E(X)dX\right) \tag{21}$$

The solutions for cake formation when the membrane resistance and gravity are significant are presented elsewhere.[4,5,25]

Case 2: cake consolidation ($\phi_0 < \phi_{cap}$ and $P_y(\phi_0) < 1$)

Beyond T_F for $\phi_0 < \phi_g$ or if $\phi_0 \ge \phi_g$, the capillary forces at the air–liquid interface cause the cake to consolidate. The scaled solids pressure at the cake surface (which gives the surface solids concentration) is equal to the scaled capillary pressure, $P_{cap}(T)$:

$$P_s(H(T),T) = P_{cap}(T) = P_y[\phi(H(T),T)] \tag{22}$$

$P_{cap}(T)$ is given by the Young-Laplace equation scaled by the applied pressure[17]:

$$P_{cap}(T) = \frac{2\gamma_{LV}}{r_{eff}(T)\Delta p} \tag{23}$$

where $r_{eff}(T)$ is the effective radius of curvature of the liquid/air menisci at the cake surface and γ_{LV} is the liquid–vapor surface tension. Fluid drainage causes $r_{eff}(T)$ to decrease and $\phi[H(T),T]$ to increase. $P_{cap}(T)$ increases until it equals the maximum capillary pressure, which, by thermodynamic arguments of wetting,[10] is:

$$P_{cap}^{max}(\phi) = \frac{\gamma_{LV}\cos\Theta\rho_s\bar{A}_s}{\Delta p}\frac{\phi}{1-\phi} \tag{24}$$

where Θ is the receding solid–liquid contact angle, ρ_s is the solids density, and $\bar{A}_s$ is the solids surface area per unit mass. The derivation of the Laplace-White equation (Eq. 24) is valid for any internal topology, providing that the network is uniformly packed in the horizontal direction, and has been used previously to successfully develop experimental methods for determining the advancing and receding contact angles of powders.[26–28]

The cake remains saturated until $P_{cap}(T) = P_{cap}^{max}(\phi)$, as the pressure required to desaturate the particle network exceeds the network strength and the cake will preferentially consolidate rather than desaturate. The solids velocity at the top of the cake equals the liquid velocity, such that:

$$\left.\frac{\partial\phi}{\partial Z}\right|_{H(T)} = 0 \tag{25}$$

Using a forward difference approximation in time, ΔT, the scaled differential equations become:

$$\frac{d\phi}{dZ} = \frac{1}{\Delta(\phi)}\left[\psi - \phi\frac{dV}{dT}\right] \tag{26}$$

$$\frac{d\psi}{dZ} = \frac{\phi - \phi^{<}}{\Delta T} \tag{27}$$

where $\phi^{<}$ is the value of ϕ at the previous time step.

The volume fraction distribution during cake consolidation is given at progressive time steps by solving Eqs. 26 and 27 from the membrane (where $\phi = \phi_\infty$ and $\psi = 0$) to the top of the cake for successive estimates of dV/dT until Eq. 25 is satisfied. An alternative is to iterate using the conservation of solids. If $\phi_\infty > \phi_{cap}$ [that is, $P_y(\phi_{cap}) < 1$], the cake consolidates until, at time T_C, $\phi(H_C,T_C) = \phi_{cap}$, and the cake begins to drain. If $\phi_\infty \le \phi_{cap}$ (that is, $P_y(\phi_{cap}) \ge 1$), the cake will consolidate to equilibrium with $\phi(H_\infty,\infty)$ approaching ϕ_∞.

Case 3: cake drainage ($P_{cap}^{max}(\phi_0) < 1$)

Beyond T_C if $\phi_0 < \phi_{cap}$ or if $\phi_0 \ge \phi_{cap}$, the cake desaturates as the applied pressure at $Z_f(T)$ exceeds the maximum capillary pressure of the material and the capillary pressure is $<P_y(\phi)$. The residual moisture content of the cake as the liquid front recedes through the porous solid phase, S_e, is the ratio of the liquid volume to the total void volume. $S_e = 1$ indicates complete saturation whereas $S_e = 0$ indicates completely dry solids. S_e is a function of the pressure at which the solid desaturates and is therefore a material property that is a function of ϕ.

This one-dimensional description of cake desaturation captures liquid draining through the saturated body, which is generally immobile [except in Case 3(a)], and ignores the two- and three-dimensional shear-dependent effects of cracking, including both internal cake cracking and detachment from the walls of the surrounding vessel. While the modeling and prediction of cracking are beyond the scope of this work, cracking can and is expected to be very important. This work also ignores evaporative effects,[12] which are only significant for long filtration times, after air breakthrough and for cake drying using hot air.

Assuming that gravity is insignificant, the solids are immobile during desaturation, such that ψ is zero throughout and the volume fraction distribution and cake height remain at $\phi_C(Z) = \phi(Z,T_C)$ and H_C, respectively. The rate of filtration is determined from the solids pressure gradient and the liquid volume.

The conservation of liquid volume, in scaled form, is:

$$\int_0^{H_C}(1-\phi_C)dZ = V(T) - V_C + \int_0^{Z_f(T)}(1-\phi_C)dZ + \int_{Z_f(T)}^{H_C} S_e(\phi_C)(1-\phi_C)dZ \tag{28}$$

where V_C is the scaled filtrate volume at T_C. Differentiating Eq. 28 with respect to T and rearranging gives:

$$\frac{dZ_f}{dT} = -\frac{1}{[1-\phi_C(Z_f)][1-S_e(\phi_C(Z_f))]}\frac{dV}{dT} \tag{29}$$

With $\psi = 0$, the scaled solids pressure gradient (Eq. 9) is:

$$\frac{\partial P_s}{\partial Z} = -\phi_C B(\phi_C)\frac{dV}{dT} \tag{30}$$

Integrating Eq. 30 with respect to Z from $P_s(0) = 1$ to $P_s(Z_f) = P_{cap}^{max}\ [\phi_c(Z_f)]$ gives:

$$\frac{dV}{dT} = \frac{1 - P_{cap}^{max}[\phi_C(Z_f)]}{I_B(Z_f)} \tag{31}$$

where $I_B(Z) = \int_0^z \phi_c B(\phi_c)dZ$, which represents the total fluid resistance in the saturated part of the bed. Substituting dZ_f/dT for dV/dT from Eq. 29 gives:

$$\frac{dZ_f}{dT} = -\frac{1 - P_{cap}^{max}[\phi_C(Z_f)]}{[1-\phi_C(Z_f)][1-S_e(\phi_C(Z_f))]I_B(Z_f)} \tag{32}$$

Equation 32 is solved using a Runge-Kutta numerical method in steps of ΔT from $Z_f(T_C) = H_C$ until $Z_f(T_D) = 0$.

Case 3(b): Drainage Only [$\phi_0 \ge \phi_{cap}$ and $P_y(\phi_0) \ge 1$]. For the case where $\phi_0 \ge \phi_{cap}$ and $P_y(\phi_0) \ge 1$, the cake does not consolidates as the applied pressure does not exceeds the network strength, and the cake remains at ϕ_0. The liquid recedes into the porous solid at a rate determined

by the permeability of the saturated cake with residual moisture due to capillary condensation. From the conservation of liquid volume, the scaled filtrate volume is:

$$V(T) = (1-\phi_0)[1-S_e(\phi_0)][1-Z_f(T)] \tag{33}$$

The rate of filtration is given by integrating the scaled solids pressure gradient (with $\psi = 0$ and $\phi = \phi_0$) from $P_s(0) = 1$ to $P_s[Z_f(T),T] = P_{cap}^{max}(\phi_0)$:

$$1 - P_{cap}^{max}(\phi_0) = \phi_0 B(\phi_0) Z_f(T) \frac{dV}{dT} \tag{34}$$

Substituting $Z_f(T)$ from Eq. 33, rearranging in terms of dV/dT and reciprocating gives:

$$\frac{dT}{dV} = \frac{\phi_0 B(\phi_0)}{1 - P_{cap}^{max}(\phi_0)} \left(1 - \frac{V(T)}{(1-\phi_0)[1-S_e(\phi_0)]}\right) \tag{35}$$

Integrating with respect to V gives an analytical expression for the time required to reach a given volume of filtrate:

$$T = \frac{\phi_0 B(\phi_0) V(T)}{1 - P_{cap}^{max}(\phi_0)} \left(1 - \frac{V(T)}{2(1-\phi_0)[1-S_e(\phi_0)]}\right) \tag{36}$$

Thus, Eq. 36 provides a method for experimentally determining the desaturation material properties. Providing that $\phi_0 \geq \phi_{cap}$ and $P_y(\phi_0) \geq 1$, the intercept of T/V vs. V gives $P_{cap}^{max}(\phi_0)$ and the slope gives $S_e(\phi_0)$. An alternative method is to differentiate the above expression with respect to V^2, giving:

$$\frac{dT}{dV^2} = \frac{\phi_0 B(\phi_0)}{2[1 - P_{cap}^{max}(\phi_0)]} \left(\frac{1}{V(T)} - \frac{1}{(1-\phi_0)[1-S_e(\phi_0)]}\right) \tag{37}$$

Thus, the slope of dT/dV^2 vs. $1/V$ gives $P_{cap}^{max}(\phi_0)$ and the intercept gives $S_e(\phi_0)$.

Case 3(a): Concurrent Consolidation and Drainage [$\phi_0 \geq \phi_{cap}$ and $P_y(\phi_0) < 1$]. For the case where $\phi_0 \geq \phi_{cap}$ and $P_y(\phi_0) < 1$, the cake consolidates and drains at the same time, as the solids pressure at the membrane exceeds the network strength and the pressure at the air–liquid interface exceeds the maximum capillary pressure. Three zones of behavior are expected:

- The consolidation zone up to $Z_c(T)$, where the solids pressure equals the compressive yield stress and the cake is compressing;
- The convection zone of constant concentration, ϕ_0, where the solids pressure is less than the yield stress {varying from $P_s[Z_c(T)] = P_y(\phi_0)$ to $P_s[Z_f(T)] = P_{cap}^{max}(\phi_0)$}; and
- The desaturation zone from $Z_f(T)$ to $H(T)$.

ϕ is constant at ϕ_0 in the convection zone, therefore, from Eq. 11, the solids flux, ψ, is a function of T only. From Eq. 9, the scaled solids pressure gradient in this zone is:

$$\frac{\partial P_s}{\partial Z} = B(\phi_0)\left(\psi(T) - \phi_0 \frac{dV}{dT}\right) \tag{38}$$

Integrating from $P_s[Z_c(T),T] = P_y(\phi_0)$ to $P_s[Z_f(T),T] = P_{cap}^{max}(\phi_0)$ and rearranging in terms of $Z_f(T)$ gives:

$$Z_f(T) = \frac{P_y(\phi_0) - P_{cap}^{max}(\phi_0)}{B(\phi_0)\left(\phi_0 \frac{dV}{dT} - \psi(T)\right)} + Z_c(T) \tag{39}$$

$H(T)$ is given by the conservation of solid volume:

$$H(T) = \frac{1}{\phi_0} \int_0^{Z_c(T)} \phi dZ + Z_c(T) \tag{40}$$

The conservation of liquid volume is:

$$1 - \phi_0 = V(T) + \int_0^{Z_c(T)} (1-\phi) dZ + \int_{Z_c(T)}^{Z_f(T)} (1-\phi_0) dZ + \int_{Z_f(T)}^{H(T)} S_e(\phi_0)(1-\phi_0) dZ \tag{41}$$

Rearranging and simplifying Eqs. 40 and 41 gives:

$$Z_f(T) = H(T) + \frac{1 - V(T) - H(T)}{[1-S_e(\phi_0)](1-\phi_0)} \tag{42}$$

For the consolidation zone at time T, Eqs. 26 and 27 are solved for an estimate of dV/dT from $Z = 0$ until $\phi = \phi_0$, giving $Z_c(T)$ and $\psi(T)$. $Z_f(T)$ is then given by Eq. 39 and checked against Eq. 42 to improve the estimate of dV/dT. Steps of ΔT are repeated until dZ_c/dT equals zero, when the cake stops consolidating and the liquid front proceeds into the cake at a rate given by Eq. 32. To the authors' knowledge, concurrent consolidation and desaturation have not been reported in the literature.

Modeling Results

The material properties of actual suspensions must be measured in the laboratory for accurate predictions of actual process performance. However, arbitrary material properties for $p_y(\phi)$, $R(\phi)$, $p_{cap}^{max}(\phi)$, and $S_e(\phi)$ have been used here for the purpose of illustrating the model formulation:

$$p_y(\phi) = 10\left[\left(\frac{\phi}{\phi_g}\right)^5 - 1\right] \text{Pa, where } \phi_g = 0.1\text{v/v} \tag{43}$$

$$R(\phi) = 10^9 (1-\phi)^{-3.5} \text{ Pa.s/m}^2 \tag{44}$$

$$p_{cap}^{max}(\phi) = 10^5 \frac{\phi}{1-\phi} \text{ Pa} \tag{45}$$

$$S_e(\phi) = 0.1 \tag{46}$$

For these properties, $\phi_{cap} = 0.353$ v/v. The model has been used to give predictions at $\phi_0 = 0.05$, 0.2, 0.36, and 0.4 v/v and $\Delta p = 4$ and 10 kPa (corresponding to $\phi_\infty = 0.332$ and 0.398 v/v, respectively), giving the six different

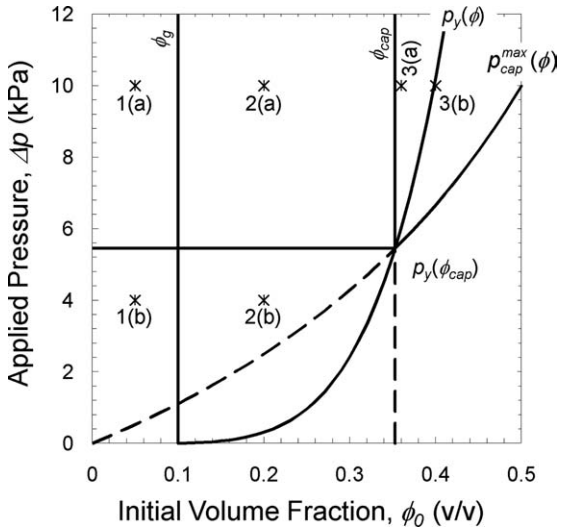

Figure 4. Applied pressure vs. initial solids volume fraction for the theoretical material.

cases outlined in the introduction (see Figure 4). The initial height is the same in all the simulations ($h_0 = 0.1$ m).

Case 1(a)

The volume fraction distribution and height vs. time results for $\phi_0 = 0.05$ v/v and $\Delta p = 10$ kPa are presented in Figure 5. The suspension is initially un-networked. The results show the cake formation process until $t_F = 45.1$ s, during which $\phi_g \leq \phi \leq \phi_\infty$ for $z \leq z_c(t)$ and $\phi[z_c(t) \leq z \leq h(t)] = \phi_0$. Beyond t_F, the cake consolidates until, at $t_C = 74.1$ s, $\phi[h(t)] = \phi_{cap}$, as the applied pressure is $>p_y(\phi_{cap})$. After t_C, the liquid front recedes into the immobile solids until $t_D = 138$ s.

Case 1(b)

The volume fraction distribution and height vs. time results for $\phi_0 = 0.05$ v/v and $\Delta p = 4$ kPa are presented in Figure 6. The results show the cake formation process until $t_F = 63.5$ s. Beyond t_F, the cake consolidates until $\phi[h(t)] = \phi_\infty$ as $\Delta p < p_y(\phi_{cap})$.

Case 2(a)

The volume fraction distribution and height vs. time results for $\phi_0 = 0.2$ v/v and $\Delta p = 10$ kPa are presented in Figure 7. The suspension is initially networked and undergoes consolidation until, at $t_C = 524$ s, $\phi[h(t)] = \phi_{cap}$. The cake is immobile after t_C. The liquid front recedes into the solids as the applied pressure is $>p_y(\phi_{cap})$, until $t_D = 1545$ s.

Case 2(b)

The volume fraction distribution and height vs. time results for $\phi_0 = 0.2$ v/v and $\Delta p = 4$ kPa are presented in Figure 8. The suspension is initially networked. As $\Delta p < p_y(\phi_{cap})$, the cake consolidates until $\phi[h(\infty)] = \phi_\infty$.

Case 3(a)

The volume fraction distribution and height vs. time results for $\phi_0 = 0.36$ v/v and $\Delta p = 10$ kPa are presented in Figure 9. As $\Delta p > p_y(\phi_0) > p_{cap}^{max}(\phi_0)$, the process undergoes concurrent cake consolidation and drainage until, at $t_C = 328$ s, $dz_c/dt = 0$. The liquid front recedes into the solids until $t_D = 3541$ s.

Case 3(b)

The fluid height vs. time results for $\phi_0 = 0.4$ v/v and $\Delta p = 10$ kPa are presented in Figure 10. As $p_y(\phi_0) > \Delta p > p_{cap}^{max}(\phi_0)$, the cake drains but does not consolidate. The predicted drainage time is $t_D = 5379$ s. The results show that the rate of filtration increases as drainage progresses, as the overall resistance of the saturated cake decreases with decreasing $z_f(t)$.

Models of incompressible cake vacuum filtration[13–15] predict that the equilibrium residual saturation is a function of the applied pressure for incompressible materials, whereas, thermodynamically, the residual moisture content is only a function of the solids concentration and the applied pressure

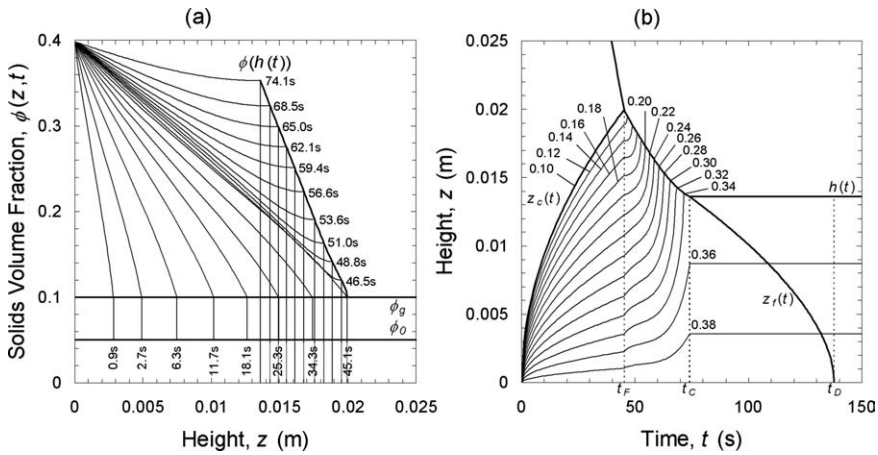

Figure 5. Numerical modeling results for Case 1(a), $\phi_0 = 0.05$ v/v, $\Delta P = 10$ kPa, and $h_0 = 0.1$ m: (a) volume fraction distribution results at a given time; (b) height vs. time results (the annotated values correspond to constant concentrations).

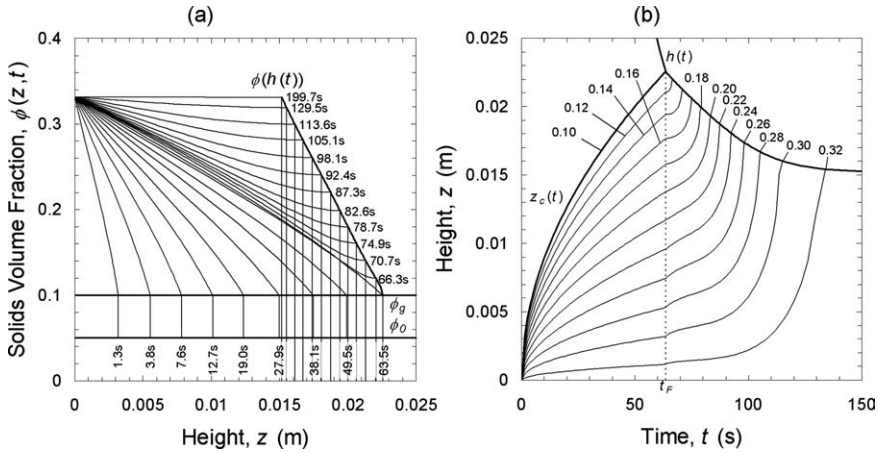

Figure 6. Numerical modeling results for Case 1(b), ϕ_0 = 0.05 v/v, ΔP = 4 kPa, and h_0 = 0.1 m: (a) volume fraction distribution results at a given time; (b) height vs. time results (the annotated values correspond to constant concentrations).

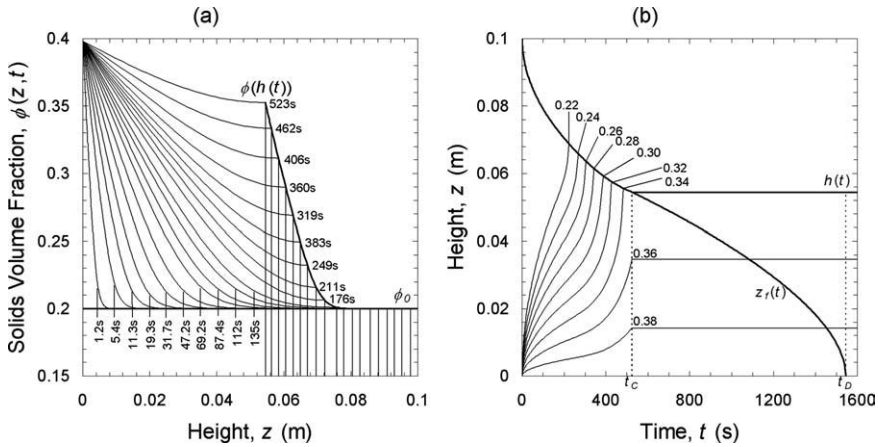

Figure 7. Numerical modeling results for Case 2(a), ϕ_0 = 0.2 v/v, ΔP = 10 kPa, and h_0 = 0.1 m: (a) volume fraction distribution results at a given time; (b) height vs. time results (the annotated values correspond to constant concentrations).

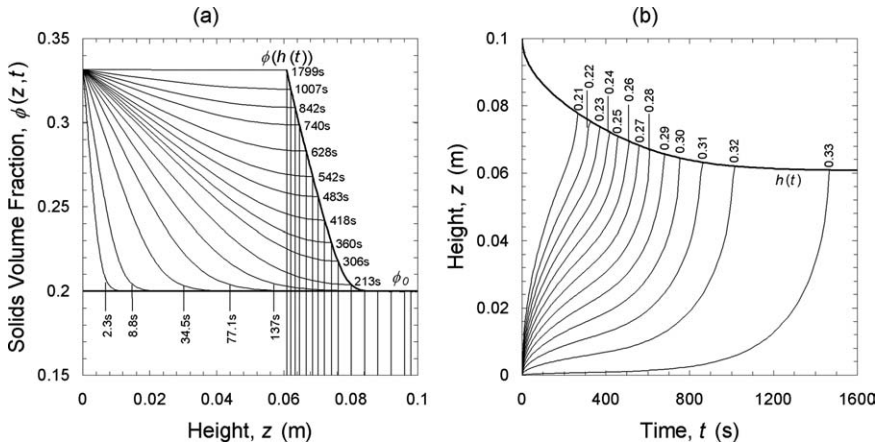

Figure 8. Numerical modeling results for Case 2(b), ϕ_0 = 0.2 v/v, ΔP = 4 kPa, and h_0 = 0.1 m: (a) volume fraction distribution results at a given time; (b) height vs. time results (the annotated values correspond to constant concentrations).

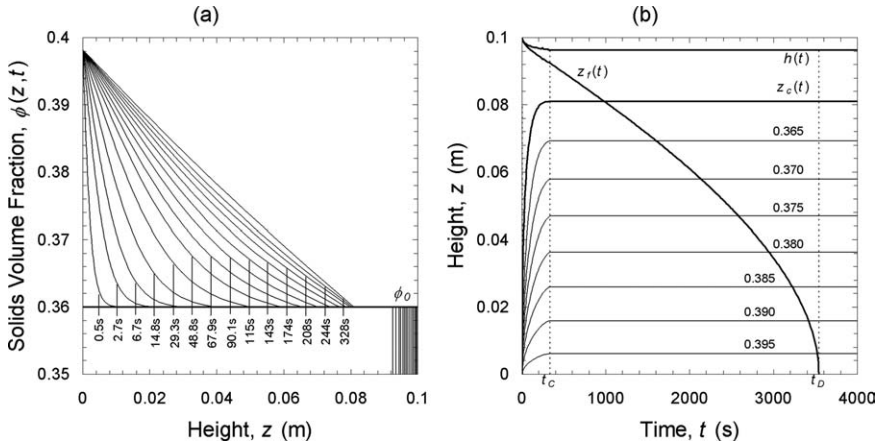

Figure 9. Numerical modeling results for Case 3(a), ϕ_0 = 0.36 v/v, ΔP = 10 kPa, and h_0 = 0.1 m: (a) volume fraction distribution results at a given time; (b) height vs. time results (the annotated values correspond to constant concentrations).

just determines the rate of filtration. Experimental results do show changes in average saturation, measured as the volume of filtrate, with pressure. This can be reconciled with the model presented here either by suggesting that cake compressibility has been ignored or that the experiment has not reached equilibrium due to cake cracking. The second phenomenon is illustrated using the model of incompressible cake drainage presented here to give average saturation as a function of time, $S(t)$, vs. applied pressure. The results for $\phi_0 = 0.4$ v/v are presented in Figure 11. Even at very large times, a pressure dependence on $S(t)$ remains.

Conclusions

A model for the one-dimensional vacuum filtration of compressible suspensions has been formulated based on compressional rheology and a numerical method outlined to solve the governing equations. Importantly, the process undergoes cake formation, consolidation, and/or desaturation depending on the initial concentration and applied pressure relative to the concentration-dependent material properties of compressive yield stress and maximum capillary pressure. A phase diagram was presented to show the interplay of these processes. The model was used in conjunction with theoretical material properties to illustrate the different types of behavior. The cake formation and consolidation components of the model have been validated, but the drainage model, while based on well-founded physics, requires experimental validation and is the subject of ongoing investigation. This work provides the necessary theoretical foundation for the experimental observations of the onset of cake drainage and the drainage rate due to one-dimensional processes.

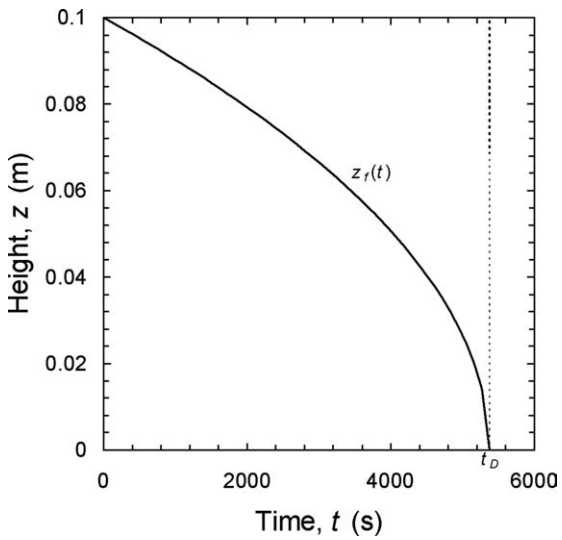

Figure 10. Numerical modeling results for Case 3(b), ϕ_0 = 0.4 v/v, ΔP = 10 kPa, and h_0 = 0.1 m.

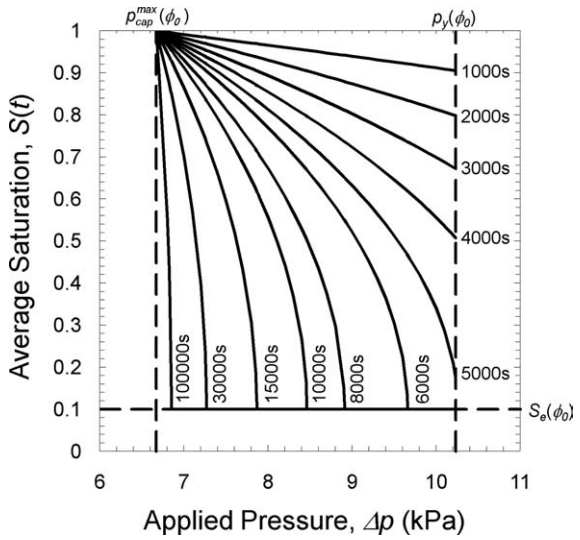

Figure 11. Modeling results of average saturation vs. applied pressure as a function of time for ϕ_0 = 0.4 v/v and h_0 = 0.1 m.

Acknowledgments

The authors acknowledge financial support by the Australian Research Council (ARC) through the Particulate Fluids Processing Centre (a Special Research Centre of the ARC) and an ARC Discovery Grant.

Literature Cited

1. Buscall R, White LR. The consolidation of concentrated suspensions. I. The theory of sedimentation. *J Chem Soc Faraday Trans 1*. 1987;83:873–891.
2. Howells I, Landman KA, Panjkov A, Sirakoff C, White LR. Time dependent batch settling of flocculated suspensions. *Appl Math Modell*. 1990;14:77–86.
3. Landman KA, White LR, Buscall R. The continuous flow gravity thickener: steady state behaviour. *AIChE J*. 1988;34:239–252.
4. Landman KA, Sirakoff C, White LR. Dewatering of flocculated suspensions by pressure filtration. *Phys Fluids A*. 1991;3:1495–1509.
5. Martin AD. Filtration of flocculated suspensions under declining pressure. *AIChE J*. 2004;50:1418–1430.
6. Stickland AD, White LR, Scales PJ. Modeling of solid-bowl batch centrifugation of flocculated suspensions. *AIChE J*. 2006;52:1351–1362.
7. Barr JD, White LR. Centrifugal drum filtration. I. A compression rheology model of cake formation. *AIChE J*. 2006;52:545–556.
8. Barr JD, White LR. Centrifugal drum filtration. II. A compression rheology model of cake draining. *AIChE J*. 2006;52:557–564.
9. Landman KA, White LR. Solid/liquid separation of flocculated suspensions. *Adv Colloid Interface Sci*. 1994;51:175–246.
10. White LR. Capillary rise in powders. *J Colloid Interface Sci*. 1982;90:536–538.
11. Brown LA, Zukoski CF. Experimental tests of two-phase fluid model of drying consolidation. *AIChE J*. 2003;49:362–372.
12. Brown LA, Zukoski CF, White LR. Consolidation during the drying of aggregated suspensions. *AIChE J*. 2002;48:492–502.
13. Wakeman RJ. Low-pressure dewatering kinetics of incompressible filter cakes. II. Constant total pressure loss or high-capacity systems. *Int J Miner Process*. 1979;5:395–405.
14. Baluais G, Dodds JA, Tondeur T. A model for the desaturation of porous media as applied to filter cakes. *Int Chem Eng*. 1985;25:436–446.
15. Nicolaou I, Stahl W. Calculation of rotary filter plants. *Aufbereit Tech*. 1992;33:328–338.
16. Wakeman RJ. Low-pressure dewatering kinetics of incompressible filter cakes. I. Variable total pressure loss or low-capacity systems. *Int J Miner Process*. 1979;5:379–393.
17. Hunter RJ. *Foundations of Colloid Science*, 2nd ed. Oxford: Oxford University Press, 2001.
18. Broadbent SR, Hammersley JM. Percolation processes. I. Crystals and mazes. *Proc Cambridge Philos Soc*. 1957;53:629–641.
19. Shante VKS, Kirkpatrick S. An introduction to percolation theory. *Adv Phys*. 1971;20:325–357.
20. Kirkpatrick S. Percolation and conduction. *Rev Mod Phys*. 1973;45:574–588.
21. Levine S, Reed P, Shutts G, Neale G. Some aspects of wetting/dewetting of a porous medium. *Powder Technol*. 1977;17:163–181.
22. Buscall R, McGowan IJ, Mills PDA, Stewart RF, Sutton D, White LR, Yates GE. The rheology of strongly-flocculated suspensions. *J Non-Newtonian Fluid Mech*. 1987;24:183–202.
23. Landman KA, White LR. Predicting filtration time and maximizing throughput in a pressure filter. *AIChE J*. 1997;43:3147–3160.
24. Matthews JH. *Numerical Methods for Mathematics, Science, and Engineering*, 2nd ed. New Jersey: Prentice-Hall, 1992.
25. Bürger R, Concha F, Karlsen KH. Phenomenological model of filtration processes. I. Cake formation and expression. *Chem Eng Sci*. 2001;56:4537–4553.
26. Dunstan D, White LR. A capillary pressure method for measurement of contact angles in powders and porous media. *J Colloid Interface Sci*. 1985;111:60–64.
27. Diggins D, Fokkink LGJ, Ralston J. The wetting of angular quartz particles: capillary pressure and contact angles. *Colloids Surf* 1990;44:299–313.
28. Prestidge CA, Ralston J. Contact angle studies of particulate sulphide minerals. *Miner Eng*. 1996;9:85–102.

Manuscript received Nov. 6, 2009, and revision received Dec. 23, 2009.